SUPPORTING INFORMATION

Crystal structure, magnetic and resonant properties of decorated spin kagome system $(CsCl)Cu_5As_2O_{10}$

Ilya V. Kornyakov,[1,2] Marina V. Likholetova,[1] Irina E. Lezova,[1] Sergey V. Krivovichev,[1,2] Harald O. Jeschke,[3,4] Yasir Iqbal,[4] Alexey V. Tkachev,[5] Sergey V. Zhurenko,[5,6] Andrey A. Gippius,[5,6] Larisa V. Shvanskaya,[6,7] Alexander N. Vasiliev[6,7]

[1]St. Petersburg State University, St. Petersburg 199034, Russia

[2]Kola Science Centre, RAS, Apatity184209, Russia

[3]Okayama University, Okayama 700-8530, Japan

[4]Department of Physics and Quantum Centre of Excellence for Diamond and Emergent Materials (QuCenDiEM), Indian Institute of Technology Madras, Chennai 600036, India

[5]Lebedev Physical Institute, RAS, Moscow, Russia

[6]Moscow State University, Moscow 119991, Russia

[7]National University of Science and Technology MISIS, Moscow 119049, Russia

1. Synthesis of $Cu_3(AsO_4)_2$

$Cu_3(AsO_4)_2$ was prepared from three reagents: $NaH_2AsO_4 \cdot H_2O$ (2 mmol; LenReactiv, 99.9 %), $CuCl_2 \cdot 2H_2O$ (1.25 mmol; LenReactiv, 99.99 %), and CuO (1.75 mmol; LenReactiv, 99.99 %). The reagents were dissolved in 443 mmol of deionized water, and the resulting solution was stirred magnetically for 30 minutes at 60 °C to ensure homogenization. The homogenized solution was then transferred into a 20 mL autoclave with a PTFE liner and heated to 200 °C in a furnace. After 7 days, the furnace was cooled at a rate of approximately 20 °C/h to room temperature. The resulting solution contained blue planar crystals. Quantitative powder X-ray diffraction analysis revealed that the final product was pure $Cu_3(AsO_4)_2$, primarily consisting of its unnamed triclinic modification (~96 %) with minor admixtures of synthetic analogues of lammerite (~3 %) and paralammerite (~1 %). The final yield was 88(2) %. The remaining material can be recovered by evaporating the solution.

2. Crystallography details

Initial screening revealed that the crystal undergoes a phase transition from trigonal to monoclinic symmetry upon cooling, accompanied by twinning. To account for this, two data collection strategies were devised, employing different exposure times (2 and 5 seconds) and detector-to-sample distances (34 and 50 mm) for the temperature ranges 400–300 K and 300–100 K, respectively. The data collection strategy for the trigonal phase was designed to acquire a hemisphere with a redundancy of 5, a frame width of 0.5°, and a 2θ angular limit of 84°. For the monoclinic phase, the strategy was adjusted with a 2θ angular limit of 76°.

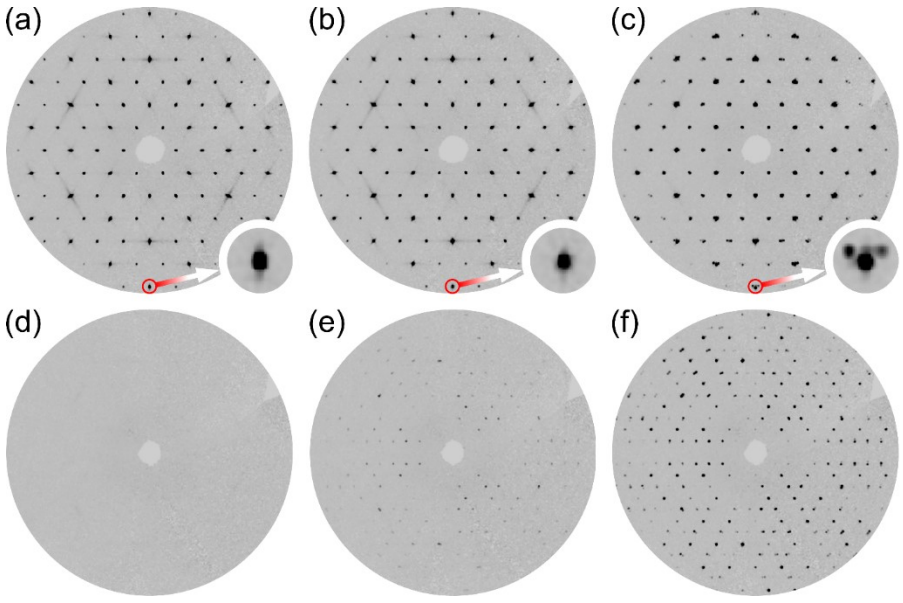

Figure S1. Reconstructed precession images of *hk*0 (**a**, **b**, **c**) and *hk*0.5 (**d**, **e**, **f**) reciprocal lattice planes (in trigonal setting) at 293 (**a**, **d**), 290 (**b**, **e**) and 280 K (**c**, **f**). Insets on (a), (b) and (c) demonstrate the shape change of $3,\bar{6},0$ reflection.

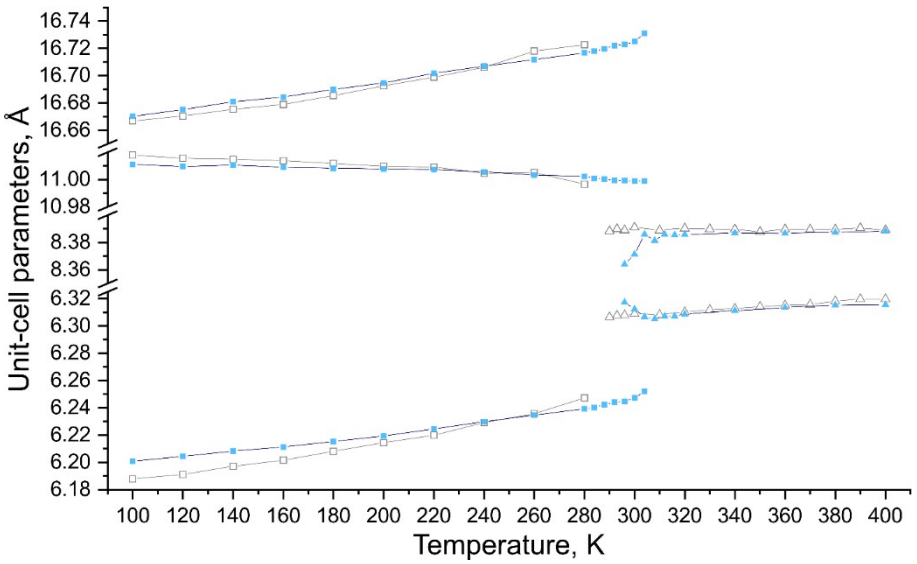

Figure S2. Changes in the unit-cell parameters of $(CsCl)Cu_5As_2O_{10}$ upon cooling according to PXRD (blue symbols) and SCXRD (empty symbols). Legend: triangles = trigonal phase; squares = monoclinic phase.

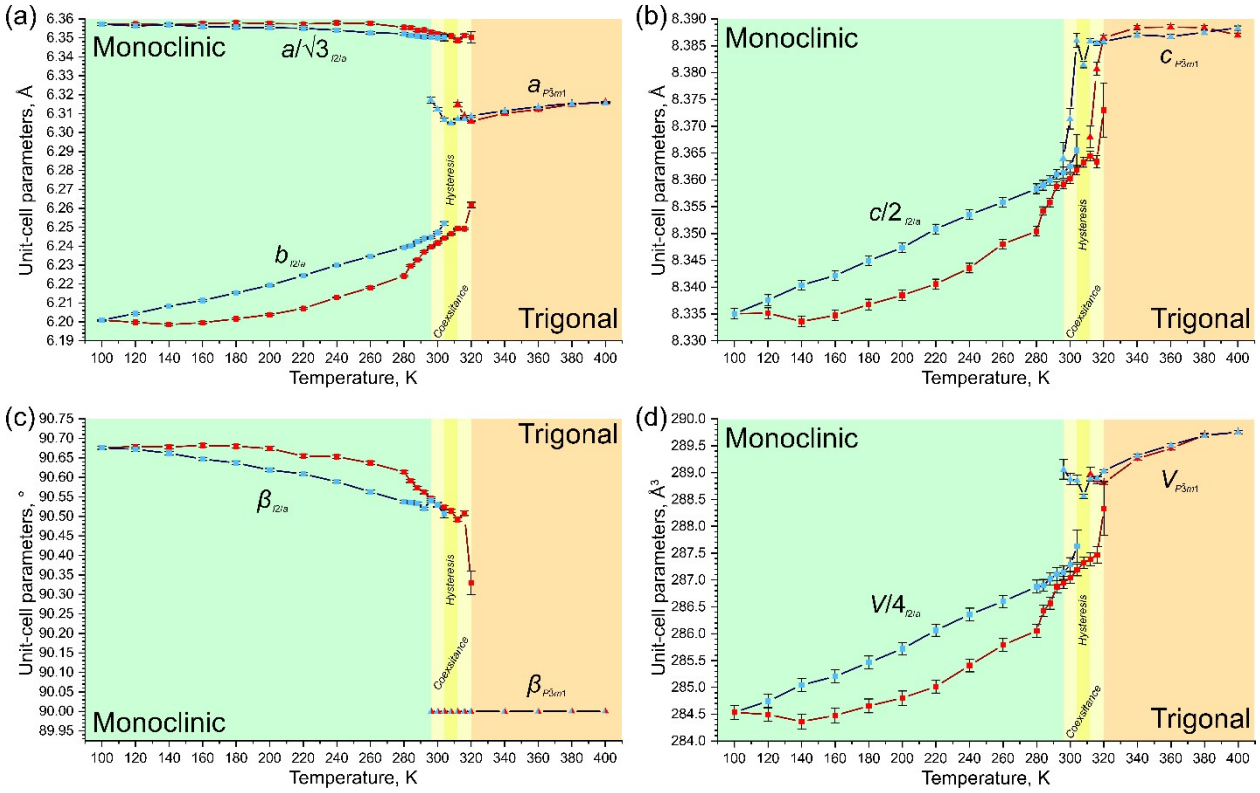

Figure S3. Changes in the (**a**) *a* and *b* parameters, (**b**) *c* parameter, (**c**) *β* parameter and (**d**) *V* parameter of $(CsCl)Cu_5As_2O_{10}$ upon cooling (blue symbols) and heating (red symbols). Legend: triangles = trigonal phase; squares = monoclinic phase.

Table S1. Selected crystallographic and refinement data for $(CsCl)Cu_5As_2O_{10}$ obtained *via* single-crystal X-ray diffraction.

T, K	Space Group	*a*, Å	*b*, Å	*c*, Å	*β*,	*V*, Å^3	R_1, wR_2, % [$F^2>2\sigma(F^2)$]	ICSD
400	$P\bar{3}m1$	6.3198(2)	= *a*	8.3891(2)	90	290.17(2)	2.34, 5.20	2480038
390		6.3198(2)	= *a*	8.3906(2)	90	290.22(2)	2.30, 5.08	2480037
380		6.3181(2)	= *a*	8.3896(2)	90	290.03(3)	2.35, 5.26	2480032
370		6.3157(3)	= *a*	8.3895(4)	90	289.81(2)	2.21, 5.09	2480039
360		6.3151(2)	= *a*	8.3897(2)	90	289.76(2)	2.27, 5.12	2480030
350		6.3142(2)	= *a*	8.3879(2)	90	289.61(2)	2.23, 5.08	2480036
340		6.3128(2)	= *a*	8.3897(2)	90	289.55(2)	2.28, 5.18	2480031
330		6.3118(2)	= *a*	8.3898(2)	90	289.46(2)	2.27, 5.31	2480033
320		6.3102(2)	= *a*	8.3903(2)	90	289.33(2)	2.37, 5.27	2480034
310		6.3081(2)	= *a*	8.3889(2)	90	289.09(2)	2.34, 5.49	2480029
300		6.3088(2)	= *a*	8.3911(2)	90	289.23(2)	2.43, 5.50	2480035
296		6.3079(1)	= *a*	8.389(2)	90	289.075(11)	2.25, 5.12	2480025
293		6.3076(1)	= *a*	8.3899(2)	90	289.078(11)	2.31, 5.23	2480027
290		6.3065(1)	= *a*	8.3884(2)	90	288.926(11)	2.32, 5.00	2480026
280	*I*2/*a*	10.9966(3)	6.2472(2)	16.7226(4)	90.503(2)	1148.76(6)	4.87, 13.44	2480028
260		11.0052(2)	6.2356(1)	16.7180(4)	90.564(2)	1147.20(4)	4.20, 12.31	2480023
240		11.0046(2)	6.2291(1)	16.7060(4)	90.580(2)	1145.12(4)	4.47, 13.02	2480024
220		11.0092(2)	6.2199(1)	16.6989(4)	90.618(2)	1143.41(4)	4.32, 12.12	2480022
200		11.0097(2)	6.2145(1)	16.6925(4)	90.622(2)	1142.03(4)	3.95, 10.97	2480021
180		11.0118(2)	6.20811(14)	16.6854(4)	90.647(2)	1140.58(4)	3.97, 11.41	2480019
160		11.0138(2)	6.20157(14)	16.6789(4)	90.662(2)	1139.15(4)	3.82, 11.21	2480020
140		11.0149(2)	6.19717(13)	16.6754(4)	90.671(2)	1138.21(4)	3.98, 11.40	2480018
120		11.0156(2)	6.19120(13)	16.6704(4)	90.678(2)	1136.84(4)	3.82, 11.07	2480017
100		11.0179(2)	6.18791(12)	16.6668(4)	90.698(2)	1136.22(4)	4.48, 13.61	2480016

Table S2. Crystallographic data for $(CsCl)Cu_5As_2O_{10}$ obtained *via* powder X-ray diffraction.

T, K	Space Group	*a*, Å	*b*, Å	*c*, Å	*β*,	*V*, Å^3	R_{wp}, %	R_{exp}, %	GOF
400	$P\bar{3}m1$	6.3156(3)	= *a*	8.3883(4)	90	289.75(3)	2.57	1.88	1.37
380		6.3152(3)	= *a*	8.3875(4)	90	289.69(3)	2.51	1.88	1.34
360		6.3135(3)	= *a*	8.3867(4)	90	289.51(3)	2.57	1.88	1.37
340		6.3113(3)	= *a*	8.3870(4)	90	289.32(3)	2.54	1.88	1.36
320		6.3086(3)	= *a*	8.3858(4)	90	289.03(3)	2.57	1.88	1.37
316		6.3072(3)	= *a*	8.3855(4)	90	288.89(3)	2.51	1.88	1.34
312		6.3071(3)	= *a*	8.3859(4)	90	288.89(3)	2.54	1.88	1.35
308		6.3051(4)	= *a*	8.3815(6)	90	288.56(4)	2.68	1.88	1.43
304	$P\bar{3}m1$ 42(1)%	6.3067(9)	= *a*	8.386(1)	90	288.86(9)	2.61	1.87	1.39
304	*I*2/*a* 58(1)	10.999(2)	6.252(1)	16.731(3)	90.51(1)	1150.5(3)	2.61	1.87	1.39
300	$P\bar{3}m1$ 21(1)%	6.3124(9)	= *a*	8.371(2)	90	288.9(1)	2.32	1.87	1.24
300	*I*2/*a* 79(1)%	10.9988(7)	6.2472(4)	16.72(1)	90.530(6)	1149.1(1)	2.32	1.87	1.24
296	$P\bar{3}m1$ 15(1)%	6.317(2)	= *a*	8.364(3)	90	289.1(2)	2.32	1.87	1.24
296	*I*2/*a* 85(1)%	10.9992(7)	6.2446(4)	16.723(1)	90.541(5)	1148.6(1)	2.32	1.87	1.24
292	*I*2/*a*	10.9995(7)	6.2441(4)	16.7220(9)	90.520(4)	1148.4(1)	2.39	1.87	1.28
288		11.0004(6)	6.2424(4)	16.7198(9)	90.533	1148.1(1)	2.44	1.87	1.30
284		11.0009(6)	6.2402(4)	16.718(9)	90.536	1147.6(1)	2.35	1.87	1.26
280		11.0024(7)	6.2393(4)	16.7167(9)	90.538	1147.5(1)	2.4	1.87	1.28
260		11.0033(6)	6.2346(4)	16.7117(9)	90.563	1146.4(1)	2.4	1.87	1.28
240		11.0056(7)	6.2299(4)	16.707(9)	90.589	1145.4(1)	2.42	1.87	1.29

220		11.0073(6)	6.2245(4)	16.7017(9)	90.609	1144.2(1)	2.39	1.88	1.28
200		11.0078(7)	6.2193(4)	16.6947(9)	90.619	1142.9(1)	2.37	1.87	1.26
180		11.0083(7)	6.2153(4)	16.6899(9)	90.637	1141.8(1)	2.46	1.87	1.31
160		11.0090(7)	6.2113(4)	16.6843(9)	90.647	1140.8(1)	2.52	1.88	1.34
140		11.0106(7)	6.2083(4)	16.6808(9)	90.662	1140.2(1)	2.56	1.88	1.36
120		11.0095(7)	6.2044(4)	16.675(1)	90.672	1139.0(1)	2.63	1.88	1.4
100		11.0111(7)	6.2009(4)	16.670(1)	90.676	1138.1(1)	2.63	1.88	1.4
120		11.0114(7)	6.1998(4)	16.670(1)	90.679	1138.0(1)	2.74	1.88	1.46
140		11.0105(8)	6.1986(5)	16.667(1)	90.678	1137.5(1)	2.8	1.88	1.49
160		11.0117(8)	6.1996(5)	16.669(1)	90.682	1137.9(1)	2.79	1.88	1.49
180		11.0124(8)	6.2016(5)	16.673(1)	90.68	1138.6(1)	2.73	1.88	1.46
200		11.0117(7)	6.2038(4)	16.677(1)	90.674	1139.2(1)	2.68	1.87	1.43
220		11.0113(7)	6.2071(4)	16.6812(9)	90.655	1140.1(1)	2.59	1.87	1.38
240		11.0123(7)	6.2129(4)	16.6871(9)	90.653	1141.6(1)	2.49	1.87	1.33
260		11.0117(7)	6.2181(4)	16.6961(9)	90.637	1143.1(1)	2.46	1.87	1.31
280		11.0082(7)	6.2242(4)	16.7008(9)	90.614	1144.2(1)	2.36	1.87	1.26
284		11.0079(6)	6.2296(4)	16.7084(8)	90.591	1145.7(1)	2.34	1.87	1.25
288		11.0055(6)	6.2328(4)	16.7116(8)	90.573	1146.3(1)	2.3	1.87	1.23
292		11.0058(6)	6.2370(4)	16.7176(8)	90.562	1147.5(1)	2.35	1.87	1.26
296		11.0038(6)	6.2396(4)	16.7183(8)	90.546	1147.8(1)	2.33	1.87	1.25
300		11.0022(6)	6.2417(4)	16.7204(9)	90.53	1148.2(1)	2.34	1.87	1.25
304		11.0010(6)	6.2442(4)	16.7237(9)	90.523	1148.7(1)	2.36	1.87	1.26
308		11.0003(6)	6.2465(4)	16.7265(9)	90.514	1149.3(1)	2.42	1.87	1.29
312	$P\bar{3}m1$ $_{20(1)\%}$	6.315(1)	= *a*	8.368(2)	90	289.0(1)	2.26	1.87	1.21
312	$I2/a$ $_{80(1)\%}$	10.9984(7)	6.2475(4)	16.726(1)	90.531(5)	1149.2(1)	2.26	1.87	1.21
316	$P\bar{3}m1$ $_{40(1)\%}$	6.3086(6)	= *a*	8.381(1)	90	288.86(7)	2.45	1.87	1.26
316	$I2/a$ $_{60(1)\%}$	11.0009(8)	6.2492(5)	16.727(1)	90.508(6)	1149.9(1)	2.45	1.87	1.26
320	$P\bar{3}m1$ $_{83(1)\%}$	6.3060(3)	= *a*	8.3865(5)	90	288.81(3)	2.45	1.87	1.31
320	$I2/a$ $_{17(1)\%}$	10.999(3)	6.262(1)	16.746(5)	90.33(3)	1153.3(5)	2.45	1.87	1.31
340	$P\bar{3}m1$	6.3102(3)	= *a*	8.3884(4)	90	289.26(3)	2.48	1.87	1.32
360		6.3122(3)	= *a*	8.3885(4)	90	289.45(3)	2.54	1.87	1.36
380		6.3149(3)	= *a*	8.3884(4)	90	289.70(3)	2.54	1.87	1.36
400		6.3160(3)	= *a*	8.3870(4)	90	289.75(3)	2.53	1.87	1.35

Table S3. Fitted expressions for the temperature dependence of unit-cell parameters of $(CsCl)Cu_5As_2O_{10}$ obtained *via* powder X-ray diffraction.

Temperature range, K	Space Group	Target unit-cell parameter	Equation	R^2
Upon cooling				
400 – 308	$P\bar{3}m1$	*a*	$6.14(2) + 9(1)T\cdot10^{-4} - 1.1(2)T^2\cdot10^{-6}$	0.98
400 – 308	$P\bar{3}m1$	*c*	$8.33(7) + 3(4)T\cdot10^{-4} - 4(5)T^2\cdot10^{-7}$	0.63
400 – 308	$P\bar{3}m1$	*V*	$270(4) + 0.10(2)T - 1.2(4)T^2\cdot10^{-4}$	0.97
288 – 100	$I2/a$	*a*	$11.007(2) + 7(2)T\cdot10^{-5} - 3.1(5)T^2\cdot10^{-7}$	0.98
288 – 100	$I2/a$	*b*	$6.190(1) + 8(2)T\cdot10^{-5} + 3.6(4)T^2\cdot10^{-7}$	0.99
288 – 100	$I2/a$	*c*	$16.648(2) + 2.1(3)T\cdot10^{-4} + 1.4(6)T^2\cdot10^{-7}$	0.99
288 – 100	$I2/a$	*β*	$90.67(1) + 3(1)T\cdot10^{-4} - 2.8(3)T^2\cdot10^{-6}$	0.99
288 – 100	$I2/a$	*V*	$1134.1(6) + 3.6(6)T\cdot10^{-2} + 4(1)T^2\cdot10^{-5}$	0.99
Upon heating				
100 – 280	$I2/a$	*a*	$11.004(4) + 9(4)T\cdot10^{-5} - 2(1)T^2\cdot10^{-7}$	0.48
100 – 280	$I2/a$	*b*	$6.223(1) - 3.5(2)T\cdot10^{-4} + 1.26(5)T^2\cdot10^{-6}$	0.99
100 – 280	$I2/a$	*c*	$16.691(5) - 3.5(6)T\cdot10^{-4} + 1.4(1)T^2\cdot10^{-6}$	0.99

100 – 280	$I2/a$	β	$90.61(1) + 1.0(2)T\cdot10^{-3} – 3.6(4)T^2\cdot10^{-6}$	0.98
100 – 280	$I2/a$	V	$1142.9(9) – 8(1)T\cdot10^{-2} + 3.0(3)T^2\cdot10^{-4}$	0.99
280 – 308	$I2/a$	a	$11.094(6) – 3.0(2)T\cdot10^{-4}$	0.97
280 – 308	$I2/a$	b	$4.8(2) + 9(1)T\cdot10^{-3} – 1.4(2)T^2\cdot10^{-5}$	0.99
280 – 308	$I2/a$	c	$14.8(6) + 1.2(4)T\cdot10^{-2} – 2.0(7)T^2\cdot10^{-5}$	0.98
280 – 308	$I2/a$	β	$96(1) – 3.9(7)T\cdot10^{-2} + 6(1)T^2\cdot10^{-5}$	0.99
280 – 308	$I2/a$	V	$756(102) + 2.5(7)T – 4(1)T^2\cdot10^{-3}$	0.98
320 – 400	$P\bar{3}m1$	a	$6.14(4) + 8(2)T\cdot10^{-4} – 10(3)T^2\cdot10^{-7}$	0.99
320 – 400	$P\bar{3}m1$	c	$8.23(2) + 9(1)T\cdot10^{-4} – 1.2(2)T^2\cdot10^{-7}$	0.96
320 – 400	$P\bar{3}m1$	V	$268(4) + 0.11(2)T – 1.3(3)T^2\cdot10^{-3}$	0.99

Note: the unit-cell parameters of coexisting phases were not taken into account.

Table S4. Selected bond lengths in trigonal $(CsCl)Cu_5As_2O_{10}$.

	Bond lengths, Å						
T, K	As1–O1	As1–O2	Cu1–O1	Cu1–O2	Cu1–O3	Cu2–O2	Cu2–O3
400	1.636(3)	1.679(2)	1.847(3)	2.105(2)	1.892(2)	2.000(2)	1.8767(5)
390	1.639(3)	1.680(2)	1.846(3)	2.105(2)	1.891(2)	2.000(2)	1.8771(5)
380	1.638(3)	1.679(2)	1.846(3)	2.104(2)	1.891(2)	2.000(2)	1.8765(5)
370	1.636(3)	1.678(2)	1.849(3)	2.103(2)	1.892(2)	2.000(2)	1.8756(5)
360	1.639(3)	1.679(2)	1.847(3)	2.103(2)	1.891(2)	2.000(2)	1.8755(5)
350	1.637(3)	1.679(2)	1.848(3)	2.102(2)	1.889(2)	1.999(2)	1.8755(5)
340	1.638(3)	1.678(2)	1.848(3)	2.102(2)	1.889(2)	1.999(2)	1.8752(5)
330	1.639(3)	1.678(2)	1.848(3)	2.101(2)	1.891(2)	2.001(2)	1.8745(5)
320	1.639(3)	1.680(2)	1.849(3)	2.099(2)	1.889(2)	1.999(2)	1.8743(5)
310	1.638(3)	1.678(2)	1.849(3)	2.099(2)	1.889(2)	1.999(2)	1.8736(5)
300	1.640(3)	1.679(2)	1.849(3)	2.098(2)	1.892(2)	2.000(2)	1.8733(5)
296	1.637(3)	1.677(2)	1.850(3)	2.100(2)	1.890(3)	1.999(2)	1.8734(6)
293	1.637(3)	1.678(2)	1.851(3)	2.099(2)	1.890(3)	2.000(2)	1.8732(6)
290	1.639(3)	1.677(2)	1.849(3)	2.099(2)	1.890(3)	2.001(2)	1.8727(6)
	Bond lengths averaged over the entire temperature range, Å						
	1.638(1)	1.679(1)	1.848(1)	2.101(2)	1.890(1)	2.000(1)	1.875(1)

Table S5. Selected bond lengths in monoclinic (CsCl)$Cu_5As_2O_{10}$.

	Bond lengths, Å														
T, K	As1–O1	As1–O2	As1–O3	As1–O4	Cu1–O1	Cu1–O2	Cu1–O3	Cu1–O4	Cu1–O5	Cu2–O2	Cu2–O3	Cu2–O5	Cu2–O5^{i}	Cu3–O4	Cu3–O5
280	1.642(4)	1.681(4)	1.695(4)	1.690(4)	1.853(4)	2.331(4)	2.024(4)	2.059(4)	1.892(3)	2.002(4)	2.024(3)	1.894(3)	1.887(3)	1.988(4)	1.880(4)
260	1.646(4)	1.678(4)	1.696(4)	1.697(4)	1.853(4)	2.356(4)	2.023(3)	2.051(4)	1.891(3)	2.007(4)	2.021(3)	1.892(3)	1.890(3)	1.982(4)	1.883(3)
240	1.649(4)	1.682(3)	1.697(3)	1.695(3)	1.854(4)	2.371(3)	2.014(3)	2.050(4)	1.892(3)	2.006(3)	2.027(3)	1.894(3)	1.889(3)	1.985(4)	1.884(3)
220	1.648(4)	1.679(4)	1.697(3)	1.694(3)	1.852(4)	2.386(4)	2.011(3)	2.052(3)	1.892(3)	2.004(4)	2.029(3)	1.899(3)	1.891(3)	1.983(4)	1.879(3)
200	1.647(3)	1.687(3)	1.701(3)	1.696(3)	1.855(3)	2.392(3)	2.008(3)	2.046(3)	1.892(3)	2.003(3)	2.028(3)	1.896(3)	1.892(3)	1.983(3)	1.884(3)
180	1.652(3)	1.682(3)	1.698(3)	1.703(3)	1.851(3)	2.407(3)	2.008(3)	2.038(3)	1.893(3)	2.003(3)	2.032(3)	1.900(3)	1.888(3)	1.978(3)	1.885(3)
160	1.651(3)	1.683(3)	1.702(3)	1.701(3)	1.855(3)	2.414(3)	2.006(3)	2.040(3)	1.900(3)	2.004(3)	2.028(3)	1.896(3)	1.891(3)	1.975(3)	1.882(3)
140	1.653(3)	1.686(3)	1.701(3)	1.704(3)	1.853(3)	2.420(3)	2.004(3)	2.036(3)	1.901(3)	2.006(3)	2.031(3)	1.898(3)	1.889(3)	1.976(3)	1.883(3)
120	1.655(3)	1.683(3)	1.701(3)	1.702(3)	1.853(3)	2.428(3)	2.001(3)	2.039(3)	1.904(3)	2.005(3)	2.032(3)	1.899(3)	1.890(3)	1.980(3)	1.880(3)
100	1.661(4)	1.680(4)	1.703(4)	1.703(4)	1.851(4)	2.436(4)	2.001(4)	2.038(4)	1.902(4)	2.008(4)	2.028(4)	1.906(4)	1.889(4)	1.977(4)	1.877(4)
	Bond lengths averaged over the entire temperature range, Å														
	1.650(5)	1.682(3)	1.699(3)	1.699(5)	1.853(1)	2.39(3)	2.010(8)	2.045(8)	1.896(5)	2.005(2)	2.028(3)	1.897(4)	1.890(2)	1.981(4)	1.882(3)

i = −x+1, y−1/2, −z+1/2

3. Additional details of the DFT energy mapping

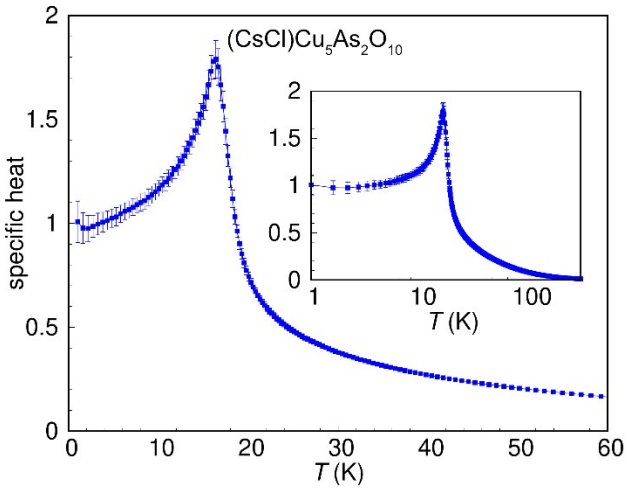

Figure S4. Classical Monte Carlo specific heat for the full Heisenberg Hamiltonian of $(CsCl)Cu_5As_2O_{10}$ comprising 20 exchange interactions. Magnetic order sets in at $T_N = 13.7$ K.

We show the detailed result of the DFT energy mapping in Fig. S5. Reading off the Hamiltonian at the U value where the couplings yield the Curie-Weiss temperature of $\theta_{CW} = -106$K, we obtain the following Hamiltonian paramters: $J_1 = 102(6)$ K (Cu1–Cu2, in-plane cap to kagome), $J_2 = 134(6)$ K (Cu2–Cu2, inplane, kagome nearest neighbor), $J_3 = -17(5)$ K (Cu1–Cu1, interlayer), $J_4 = -25(4)$ K (Cu1–Cu2, in-plane cap to kagome), $J_5 = -2(6)$ K (Cu2–Cu2, in-plane kagome second neighbor), $J_6 = 38(8)$ K (Cu1–Cu1, cap to cap), $J_{7a} = 0(4)$ K (Cu2–Cu2, kagome third neighbor), $J_{7b} = 1(4)$ K (Cu2-Cu2, kagome third neighbor across hexagon), $J_8 = 54(3)$ K (Cu1–Cu2 interlayer), $J_9 = -16(5)$ K (Cu1–Cu2 in-plane cap to kagome), $J_{10} = 0(3)$ K (Cu1–Cu2 interlayer), $J_{11} = -13(4)$ K (Cu1–Cu1 interlayer), $J_{12} = -18(7)$ K (Cu1–Cu2 in-plane cap to kagome), $J_{13} = 0(3)$ K (Cu2–Cu2 in-plane), $J_{14} = 0(4)$ K (Cu2–Cu2 interlayer), $J_{15} = -11(5)$ K (Cu1–Cu1 interlayer), $J_{16} = 2(2)$ K (Cu1–Cu2 interlayer), $J_{17} = 1(4)$ K (Cu2–Cu2 interlayer), $J_{18} = 1(3)$ K (Cu1–Cu2 in-plane cap to kagome), $J_{23} = -1(4)$ K (Cu1–Cu2 in-plane cap to kagome).

In the energy mapping procedure, we need to determine the overall energy scale of the exchange interactions as given by the Curie-Weiss temperature in order to fix the interaction parameter U. We use a fitting ansatz developed recently by Pohle and Jaubert [S1] for spin liquids:

$$\chi T\Big|^{\text{fit}} = \frac{1 + b_1 \exp[c_1/T]}{a + b_2 \exp[c_2/T]}$$
$$C = \frac{1 + b_1}{a + b_2}, \quad \theta_{\text{CW}} = \frac{b_1 c_1}{1 + b_1} - \frac{b_2 c_2}{a + b_2} \qquad \text{(S1).}$$

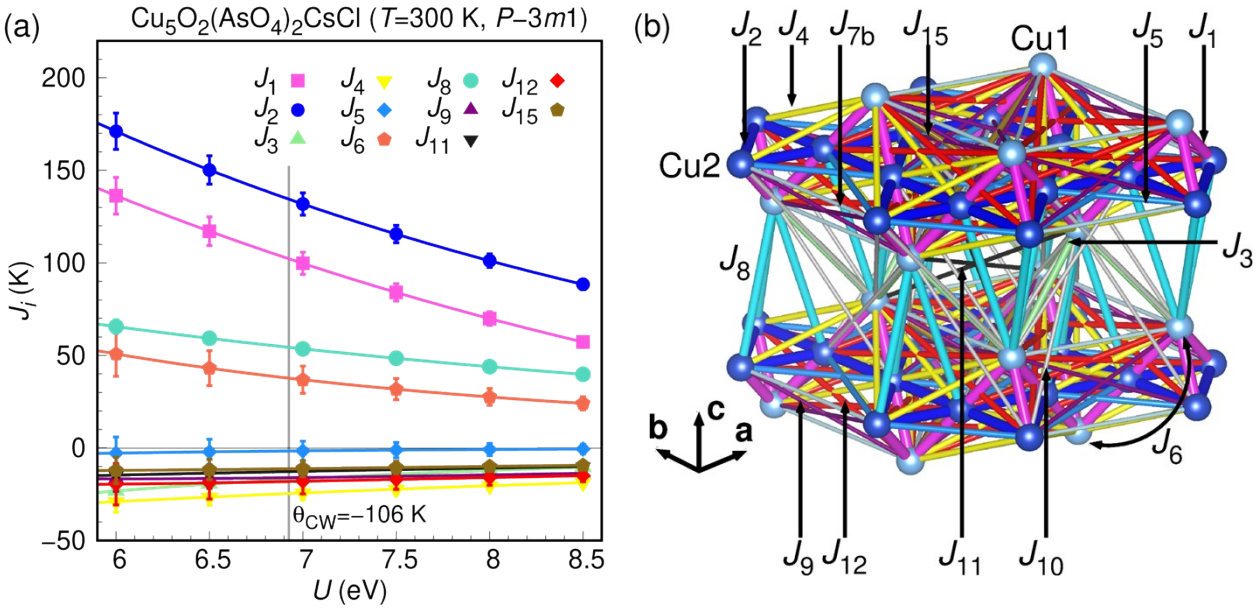

Figure S5. Detailed result of the DFT energy mapping approach. Some longer range exchange interaction within and between the layers are ferromagnetic.

The fit is shown in Fig. S6. It is excellent right down to 25 K and allows us to determine the Curie-Weiss temperature of As-averievite to $\theta_{CW} = -106$ K. Note that by evaluating the energy mapping results at this Curie-Weiss temperature, the largest couplings $J_1 = 102$ K and $J_2 = 134$ K coincide with the temperature T ~ 130K at which the susceptibility shows a broad maximum indicating the onset of short-range correlations.

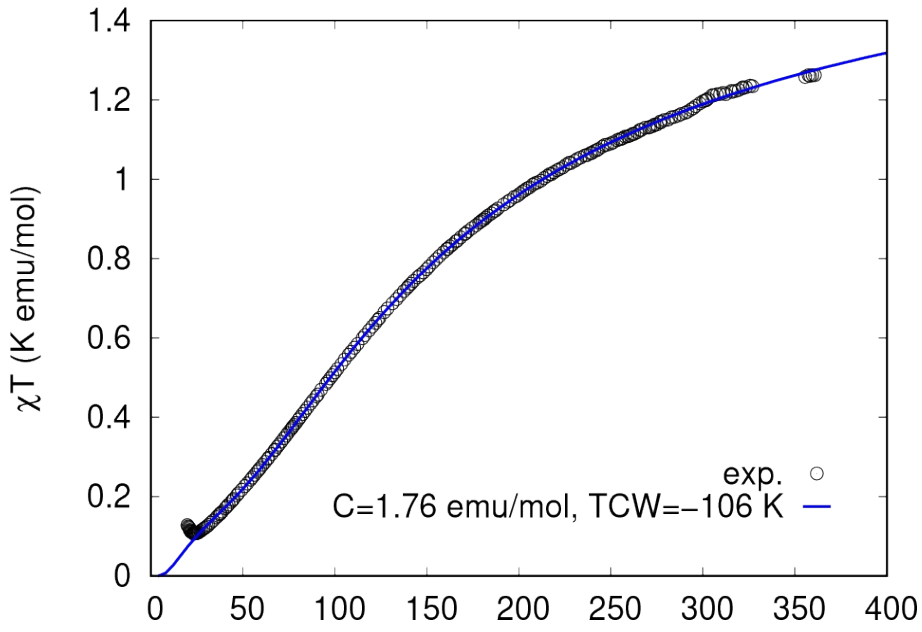

Figure S6. Magnetic susceptibility $\chi(T)$ of As-averievite, multiplied by temperature (symbols) and fit by the ansatz of Eq. (S1).

Table S6. Exchange interactions of As-Averievite obtained by DFT energy mapping. The line in bold face corresponds to the set of couplings that match the experimental Curie-Weiss temperature.

U (eV)	J_1 (K)	J_2 (K)	J_3 (K)	J_4 (K)	J_5 (K)	J_6 (K)	J_{7a} (K)	J_{7b} (K)	J_8 (K)	J_9 (K)
5.5	158(13)	195(13)	-28(11)	-32(8)	-4(12)	60(16)	1(7)	0(7)	73(5)	-17(9)
6	136(10)	171(10)	-23(8)	-29(6)	-3(9)	51(13)	1(5)	0(6)	66(4)	-17(7)
6.192	**129(9)**	**163(9)**	**-22(8)**	**-28(6)**	**-3(9)**	**48(12)**	**0(5)**	**0(6)**	**63(4)**	**-17(7)**
6.5	117(8)	150(8)	-20(7)	-27(5)	-2(7)	43(10)	0(4)	0(5)	59(3)	-16(6)
7	100(7)	132(6)	-17(5)	-24(4)	-2(6)	37(8)	0(4)	1(4)	54(3)	-16(5)
7.5	84(5)	116(5)	-14(4)	-22(3)	-1(5)	32(6)	0(3)	1(3)	48(2)	-15(4)
8	70(4)	101(4)	-12(3)	-20(3)	-1(4)	28(5)	-1(2)	1(2)	44(2)	-15(3)
8.5	57(3)	88(3)	-10(3)	-19(2)	-1(3)	24(4)	-1(2)	1(2)	40(2)	-14(2)
d_{Cu-Cu}(Å)	2.956	3.153	5.215	5.350	5.462	5.912	6.307	6.307	6.239	6.965

U (eV)	J_{10} (K)	J_{11} (K)	J_{12} (K)	J_{13} (K)	J_{14} (K)	J_{15} (K)	J_{16} (K)	J_{17} (K)	J_{18} (K)	J_{23} (K)	θ_{CW} (K)
5.5	0(5)	-16(8)	-20(15)	1(6)	0(7)	-12(10)	3(4)	2(8)	3(5)	-3(7)	-178
6	0(4)	-15(6)	-20(12)	1(5)	0(6)	-12(8)	3(3)	1(6)	2(4)	-2(6)	-149
6.192	**0(4)**	**-14(6)**	**-19(11)**	**0(5)**	**0(6)**	**-12(8)**	**2(3)**	**1(6)**	**2(4)**	**-2(6)**	**-139**
6.5	0(3)	-14(5)	-19(9)	0(4)	0(4)	-12(6)	2(3)	1(5)	2(3)	-2(4)	-124
7	0(3)	-13(4)	-18(7)	0(3)	0(4)	-11(5)	2(2)	1(4)	1(3)	-1(4)	-103
7.5	0(2)	-12(3)	-17(6)	0(3)	0(3)	-11(4)	1(2)	1(3)	1(2)	-1(3)	-85
8	1(2)	-11(3)	-16(5)	0(2)	0(2)	-10(3)	1(2)	1(3)	1(2)	-1(2)	-67
8.5	1(1)	-10(2)	-15(4)	0(2)	0(2)	-9(3)	1(1)	1(2)	1(2)	-1(2)	-55
d_{Cu-Cu}(Å)	7.743	8.183	8.270	8.343	8.391	8.644	8.935	8.963	9.396	10.400	

REFERENCES

[S1] Pohle, R.; Jaubert, L. D. C. Curie-law crossover in spin liquids. *Physical Review B* **2023**, *108*, 024411. DOI: 10.1103/PhysRevB.108.024411